Safe Swerve Maneuvers for Autonomous Driving

Ryan De Iaco, Stephen L. Smith, and Krzysztof Czarnecki

***Abstract*— This paper characterizes safe following distances for on-road driving when vehicles can avoid collisions by either braking or by swerving into an adjacent lane. In particular, we focus on safety as defined in the Responsibility-Sensitive Safety (RSS) framework. We extend RSS by introducing swerve maneuvers as a valid response in addition to the already present brake maneuver. These swerve maneuvers use the more realistic kinematic bicycle model rather than the double integrator model of RSS. We show that these swerve maneuvers allow a vehicle to safely follow a lead vehicle more closely than the RSS braking maneuvers do. The use of the kinematic bicycle model is then validated by comparing these swerve maneuvers to swerves of a dynamic single-track model. The analysis in this paper can be used to inform both offline safety validation as well as safe control and planning.**

I. Introduction

The main bottleneck for the public acceptance and ubiquity of autonomous driving is the current lack of safety guarantees. One approach to establish the safety of an autonomous vehicle is to gather crash statistics from on-road driving. However, the amount of kilometers required to establish statistically significant rates can render this method impractical [1]. An alternative approach is to use simulation to test a representative set of situations that model the driving task [2]. Unfortunately, it can be difficult to capture all of the challenges associated with driving when constructing such a set [3]. A third approach for verifying the safety of a system is formally proving the behavior of a vehicle is safe [1], [4]–[6]. In order to compute useful safety bounds, this approach often includes simplifying assumptions. The difficulty with this method lies in selecting reasonable assumptions to make. Generally, the stronger the assumptions made, the easier to prove the system is safe. However, if the assumptions are too strong, they may not hold in general driving scenarios. An additional challenge with this method is that to prove safety, the driving behavior may need to be conservative, or highly restrictive.

This paper aims to address the latter issue, especially as it pertains to the Responsibility-Sensitive Safety (RSS) framework [1]. Fundamental to the RSS framework is its assumption of responsibility, and that vehicles have a duty of care to one another. The assumption of responsible behavior allows for the autonomous vehicle to make meaningful progress in the driving task. Under other frameworks that assume adversarial vehicles, the autonomous vehicle often exhibits over-conservative behavior that impedes progress.

This work was supported by the Government of Ontario.

The authors are with the Department of Electrical and Computer Engineering, University of Waterloo, Waterloo ON, N2L 3G1, Canada (ryan.deiaco@uwaterloo.ca; stephen.smith@uwaterloo.ca, kczarnec@gsd.uwaterloo.ca)

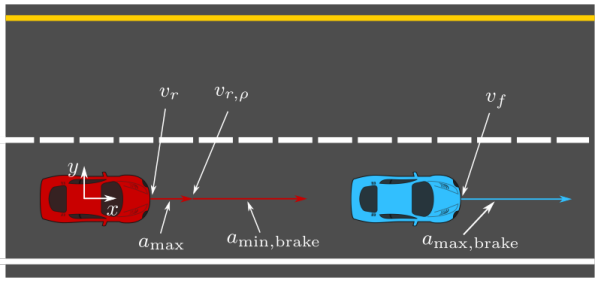

(a)

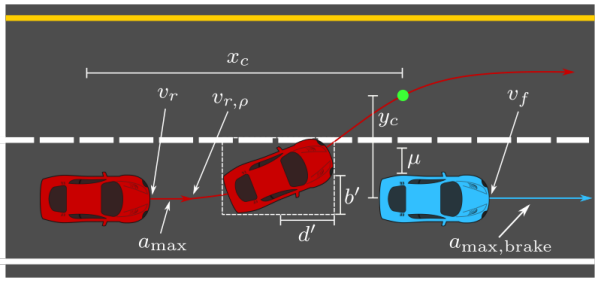

(b)

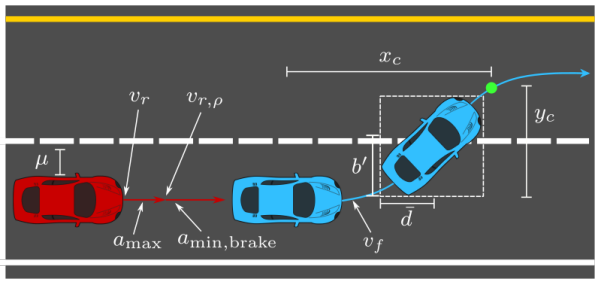

(c)

Fig. 1: (a) The standard RSS braking maneuver for a braking leading vehicle. Velocity and acceleration arrows point to path segments where they occur. The coordinate frame origin is the center of the lane at the rear vehicle's initial location. (b) The proposed swerve maneuver for a leading braking vehicle. The green dot represents the lateral clearance distance y_c required by RSS. (c) The braking maneuver required for a swerving leading vehicle.

This assumption of responsible behavior allows for the computation of safe following distances such that vehicles can comfortably brake for a braking vehicle in front of them, without causing a collision. This following distance is a function of both vehicles' speeds and maximum accelerations, as well as the reacting vehicle's reaction time. When computing this following distance, the vehicles are modeled by a kinematic particle model. If all vehicles follow the RSS framework and maintain this following distance, no collisions can occur.

This paper extends the analysis in the RSS framework to include swerve maneuvers feasible for the kinematic bicycle model. In particular, we analyze pairwise safety between swerving and braking agents. Using swerve maneuvers feasible for the kinematic bicycle model ensures that these maneuvers are more realistic than those possible under the particle model used in RSS. The simplicity of the bicycle model also allows for closed form solutions in our safe following distance bounds. This work then shows that these swerve maneuvers require less clearance to avoid collision with a lead vehicle than the braking maneuvers in the RSS framework.

A. Contributions

The contributions in this paper are as follows. The first is the derivation of closed form safe following distances in scenarios where vehicles perform swerve maneuvers that are feasible for the kinematic bicycle model. These safe following distances ensure pairwise safety between swerving and braking agents. To show pairwise safety, in addition to the scenario of braking for a braking vehicle considered in RSS, we consider the additional scenarios of swerving for a braking vehicle and braking for a swerving vehicle.

The second contribution is a validation of our use of the kinematic bicycle model by comparing our swerve maneuvers to maneuvers generated under a dynamic single-track model [7]. As part of this dynamic model, we include a Pacejka tire model [8] to account for road surface traction. We show that the kinematic model, when lateral acceleration is constrained, can form an accurate upper bound on the longitudinal distance required to perform swerve maneuvers using the dynamic model.

B. Related Work

Previous work on swerve maneuvers for autonomous driving have often focused on feasible maneuvers according to various kinodynamic models [9]. In particular, many of these papers have assumed some variant of the bicycle model [10]–[13] and performed optimization to generate optimal swerve maneuvers. However, under these models the optimal solution is not generated through a closed form solution, which makes formally proving safety challenging.

Other work has instead simplified the vehicle model to a point mass model [14]–[16] in order to yield closed form, optimal solutions. However, this comes at the cost of the nonholonomic constraint present in the bicycle model, which results in maneuvers that would be unrealistic for a car to execute. The goal with this work is to yield closed form, feasible solutions to swerve maneuver boundary condition problems, while still preserving the kinematic constraints that allow the maneuver to be executable by a real vehicle.

Previous work on using the kinematic bicycle model for autonomous driving has shown it is an effective model for tracking trajectories in MPC [17], and as such, contains important kinematic constraints that capture some of the limits of vehicle motion. Past work has also shown that the kinematic bicycle model is an accurate approximation to vehicle motion at low accelerations [18], which we expect to see as well in our validation.

II. Preliminaries

A. Responsibility-Sensitive Safety (RSS)

In this paper, we rely on two aspects of the RSS framework; the longitudinal and lateral safe distances required between two vehicles. In particular, we examine how the longitudinal safe distance for a swerve maneuver compares to that of a brake maneuver, while maintaining an appropriate lateral safe distance when required. In this work, we compare swerve maneuvers moving to the left as in Figure 1 (safe distances are computed for the red car), however, the same analysis applies to swerves moving to the right.

In RSS, safe distances are a function of several variables that describe the situation. The initial speed of the rear autonomous vehicle is given by v_r, and the initial speed of the front vehicle is denoted by v_f. The reaction time is given by ρ. The interpretation of the reaction time is the duration after which a vehicle can apply a mitigating action. During the reaction time, both vehicles apply the most dangerous acceleration possible, $a_{\max,\text{accel}}$, $a_{\max,\text{brake}}$ in the longitudinal case, and $a^{\text{lat}}_{\max}$ in the lateral case. To ensure passenger comfort, as well as to prevent tailgater safety issues, the mitigating reaction of the rear vehicle is assumed to be a comfortable deceleration, denoted $a_{\min,\text{brake}}$. This term comes from RSS, and is interpreted as the threshold for a safe, responsible braking response for the autonomous car. Note that these accelerations are magnitudes.

We denote the positive part of an expression with $[\cdot]_+$. Velocities are signed according to Figure 1a, and accelerations are unsigned parameters of the framework. If the post-reaction speeds $v_{r,\rho}$ and $v_{f,\rho}$ are given by

$$v_{r,\rho} = v_r + a_{\max,\text{accel}}\rho, \tag{1}$$

$$v^{\text{lat}}_{r,\rho} = v^{\text{lat}}_r - a^{\text{lat}}_{\max}\rho, \tag{2}$$

$$v^{\text{lat}}_{f,\rho} = v^{\text{lat}}_f + a^{\text{lat}}_{\max}\rho, \tag{3}$$

the *longitudinal and lateral safe distances* are given by

$$d_{\text{long}} = \left[v_r\rho + \frac{1}{2}a_{\max,\text{accel}}\rho^2 + \frac{v_{r,\rho}^2}{2a_{\min,\text{brake}}} - \frac{v_f^2}{2a_{\max,\text{brake}}} \right]_+, \tag{4}$$

$$d_{\text{lat}} = \mu + \left[-\left(\frac{v^{\text{lat}}_r + v^{\text{lat}}_{r,\rho}}{2} \right)\rho + \frac{(v^{\text{lat}}_{r,\rho})^2}{2a^{\text{lat}}_{\min}} + \frac{v^{\text{lat}}_f + v^{\text{lat}}_{f,\rho}}{2}\rho + \frac{(v^{\text{lat}}_{f,\rho})^2}{2a^{\text{lat}}_{\min}} \right]_+. \tag{5}$$

The longitudinal safe distance is between the frontmost point of the rear vehicle and the rearmost point of the front vehicle along the longitudinal direction, and the lateral safe distance is between the rightmost point of the rear vehicle and the leftmost point of the front vehicle along

the lateral direction. These are left implicit in the original RSS formulation, but since swerves involve rotation of the chassis, we make them explicit in this work. The longitudinal safe distance d_{long} is the distance required such that the rear vehicle can maximally accelerate during its reaction time, then minimally decelerate to a stop, all while the front vehicle is maximally braking, without causing a collision. The lateral safe distance d_{lat} is the distance required such that both vehicles can maximally accelerate towards each other during the reaction time ρ, then minimally decelerate until zero lateral velocity, while still maintaining at least a μ distance buffer.

To ensure safety for swerve maneuvers, the vehicle must maintain these safe distances with other relevant vehicles. These vehicles are relevant according to longitudinal and lateral adjacency, as defined below. We denote the vehicle dimensions d_f, d_r, b_l, b_r as in Figure 3a. We assume all vehicles have the same dimensions for simplicity, but this can be easily generalized.

Definition II.1. If x_1, x_2 denote the longitudinal position of each vehicle, and then the vehicles are *laterally adjacent* if $x_2 - d_r - d_f \leq x_1 \leq x_2 + d_r + d_f$.

Definition II.2. If y_1, y_2 denotes the lateral position of each vehicle, then the vehicles are *longitudinally adjacent* if $y_2 - b_l - b_r - d_{lat} \leq y_1 \leq y_2 + b_l + b_r + d_{lat}$.

Combining the definitions for safe distances and adjacency gives us a definition of safety.

Definition II.3. A vehicle is *laterally/longitudinally safe* from another vehicle if it is not laterally/longitudinally adjacent to the other vehicle, or if it is laterally/longitudinally adjacent to the other vehicle and there is at least d_{lat}/d_{long} of distance between them.

Definition II.4. For a swerving vehicle and a non-swerving vehicle, as well as a given swerve maneuver, we define the *lateral clearance distance*, y_c, as the earliest point in the swerve at which the swerving vehicle is no longer longitudinally adjacent to the non-swerving vehicle.

In Figure 1, y_c is reached at the green dot along the swerve. The lateral clearance distance allows us to compute the longitudinal distance covered by the swerve, which is denoted by x_c. We then use x_c to compute the equivalent of d_{long} for a swerve maneuver, and compare it to Equation (4).

B. Vehicle Models

The analysis in this paper relies upon three different kinodynamic models. The first is the particle kinematic model, which is used in the RSS framework. Through all of these kinodynamic models, x is longitudinal displacement and y is lateral displacement. The control input is the acceleration in each dimension

$$\ddot{x} = a_x, \qquad \ddot{y} = a_y. \tag{6}$$

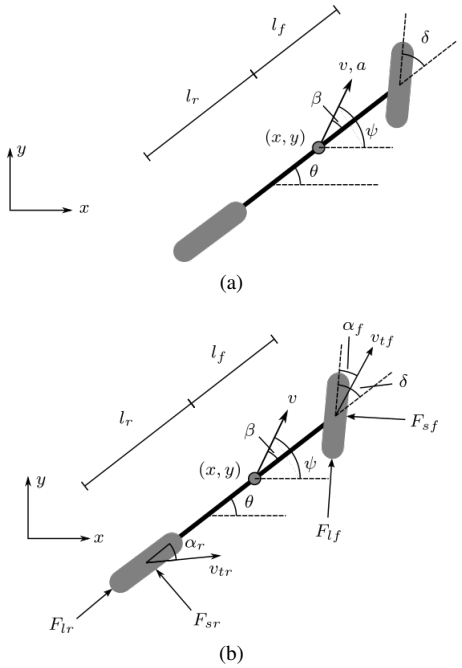

Fig. 2: (a) The kinematic bicycle model, along with its associated variables. (b) The dynamic single track model used for validation [7]. Drag forces are omitted for simplicity, but are included in our computation.

When computing swerve maneuvers, we wish to model the non-holonomic constraints on a car's motion to make the maneuvers realistic. To do so, we rely on the kinematic bicycle model, a model commonly used in autonomous driving [17], [19], [20]. This is illustrated in Figure 2a. In this model, v is the velocity of the vehicle, ψ is the heading of velocity at the centre of mass, θ is the yaw of the chassis, β is the slip angle of the centre of mass relative to the chassis, a is the input acceleration, δ is the input steering angle, R_c is the turning radius of the centre of mass, and l_r and l_f are the distances from the rear and front axle to the centre of mass, respectively

$$\begin{aligned}
&\dot{x} = v\cos(\psi+\beta), && \beta = \tan^{-1}\left(\frac{l_r}{l_r+l_f}\tan(\delta)\right),\\
&\dot{y} = v\sin(\psi+\beta), && \theta = \psi - \beta,\\
&\dot{\theta} = \frac{v\tan(\delta)}{l_r+l_f}, && |\delta| \leq \delta_{\max}\\
&\dot{v} = a, && |a_{\text{lat}}| = \frac{v^2}{R_c} \leq a^{\text{lat}}_{\min},\\
&R_c = \frac{l_r+l_f}{\cos(\beta)\tan(\delta)}, && -a_{\text{brake,min}} \leq a \leq a_{\max}.
\end{aligned} \tag{7}$$

Finally, to verify our kinematic approximation is valid, we compare our swerve maneuvers to those executed by a dynamic single-track vehicle model [7] with tires modelled using the Pacejka tire model [8]. This model is shown in Figure 2b. In this vehicle model, v, ψ, β, δ, l_f, and l_r are the same as the bicycle model. The slip angles of the front and rear tires are α_f and α_r, respectively. The lateral

tire forces on the front and rear tires are denoted F_{sf} and F_{sr}, respectively, and F_{lf} and F_{lr} denote the longitudinal tire forces at the front and rear tires, respectively. The drag mount point is denoted e_{SP}, and F_{Ax} and F_{Ay} are the longitudinal and lateral drag forces, respectively. The yaw rate is ω_z, and ω_δ is the input steering rate. The mass of the car is m, and I_{zz} is the inertia about the z-axis. We omit the equations of motion for brevity, but they are presented in the reference [7].

III. Problem Formulation

The fundamental problem this paper addresses is to compute the longitudinal safe distance required when there is a free lane (or shoulder) to the left or right of the vehicle, allowing for an evasive swerve maneuver. This requires knowing the longitudinal safe distance required for the scenarios illustrated in Figure 1. As can be seen, when computing the longitudinal safe distances for swerves, one needs to consider both longitudinal and lateral clearance, since swerves involve lateral and longitudinal displacement.

Since vehicles rotate during swerves, rotation must be compensated for when computing these clearances. After compensating for rotation, the longitudinal swerve distance x_c can then be used to compute the longitudinal safe distance required for a swerve. In RSS, safety was proved for a particle model. This paper extends those results to prove the safety for swerves feasible for the kinematic bicycle model. Section V then shows how this result can be applied to more general models. This task then breaks down into three subproblems.

Subproblem 1. Given the initial speed of a swerving vehicle v_r, the vehicle dimensions d_f, d_r, b_l, b_r as in Figure 3a, and parameters μ and ρ, compute a lateral clearance distance y_c sufficient for lateral safety when a swerving vehicle becomes laterally adjacent to a lead vehicle.

Subproblem 2. Given the kinematic constraints in (7), the initial vehicle speeds v_r and v_f, the lateral clearance distance y_c, and parameters ρ, $a_{\max}$, $a_{\min,\text{brake}}$, $a_{\max,\text{brake}}$, $a^{\text{lat}}_{\max}$, and $a^{\text{lat}}_{\min}$, compute a longitudinal safe distance sufficient for safety when swerving for a braking lead vehicle. This is illustrated in Figure 1b.

Subproblem 3. Given the initial vehicle speeds v_r and v_f, the clearance point y_c, and parameters ρ, $a_{\max}$, $a_{\min,\text{brake}}$, $a^{\text{lat}}_{\max}$, and $a^{\text{lat}}_{\min}$, compute a longitudinal safe distance sufficient for safety when braking for a swerving lead vehicle. This is illustrated in Figure 1c.

The first subproblem is addressed in Section IV-A, the second in Section IV-B, and the the third in Section IV-C.

The work in this paper makes the following assumptions on responsible behavior:

1) A vehicle will only perform a swerve maneuver if it is not braking, and will only perform a brake maneuver if it is not swerving.
2) For every swerve maneuver, each vehicle reaches the lateral clearance distance only once. As a result, once a vehicle has committed to a lane change by reaching the lateral clearance distance, it will not return to its previous lane.
3) Each vehicle moves forward along the road, $v \geq 0$ and $\frac{-\pi}{2} \leq \psi \leq \frac{\pi}{2}$.

IV. Computing the Longitudinal Safe Distance

A. Lateral Clearance Distance

To compute the lateral clearance distance y_c, we modify Equation (5) to account for vehicle rotation. If we know the maximum chassis yaw $\theta_{\max}$ during the maneuver, we can compute an axis-aligned bounding rectangle as an outer approximation to the vehicle footprint. This is useful for safety analysis, as we can now bound the swept area during the maneuver, and it is illustrated in Figure 3a.

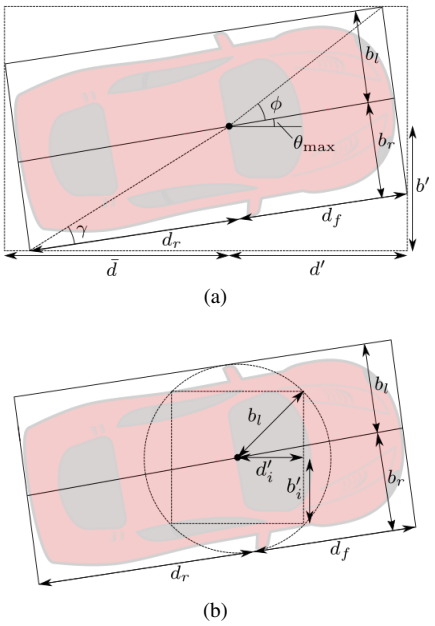

Fig. 3: (a) An outer approximation to a vehicle chassis that rotates by $\theta_{\max}$. The distances d' and $\bar{d}$ are used for longitudinal buffers during swerve maneuvers, and b' is used as a lateral buffer. (b) An inner approximation to a rotating vehicle chassis.

The three distances we need for safety analysis are from the centre of mass to the front of the bounding rectangle, d', from the centre of mass to the side of the bounding rectangle, b', and from the centre of mass to the rear of the bounding rectangle, $\bar{d}$. The distances from the centre of mass to the rear and front of the chassis are d_r and d_f, respectively. The distances to the left and right of the chassis are b_l and b_r, respectively. As the vehicle rotates, the length and width of the bounding rectangle increases until $\theta_{\max}$ reaches the angles from the centre of mass to the corners of the rectangle. Further rotation past these points decreases the dimensions of the bounding rectangle. We can write these angles in terms of ϕ and γ, illustrated in Figure 3a. The equations for the bounding rectangle distances are then d', $\bar{d}$, and b' are

$$d' = \begin{cases} d_f \cos(\theta_{\max}) + b_r \sin(\theta_{\max}) & \theta_{\max} \leq \phi, \\ \sqrt{d_f^2 + b_r^2} & \theta_{\max} > \phi, \end{cases} \tag{8}$$

$$\bar{d} = \begin{cases} d_r \cos(\theta_{\max}) + b_l \sin(\theta_{\max}) & \theta_{\max} \leq \gamma, \\ \sqrt{d_r^2 + b_l^2} & \theta_{\max} > \gamma, \end{cases} \tag{9}$$

$$b' = \begin{cases} d_r \sin(\theta_{\max}) + b_r \cos(\theta_{\max}) & \theta_{\max} \leq \frac{\pi}{2} - \gamma, \\ \sqrt{d_r^2 + b_r^2} & \theta_{\max} > \frac{\pi}{2} - \gamma. \end{cases} \quad (10)$$

We now have an expression for the bounding rectangle distances of a rotating vehicle in terms of $\theta_{\max}$, which is computed in Section IV-B.

Using b' and the lateral safe distance d_{lat}, we can now compute the lateral clearance distance, y_c required for Subproblem 1.

$$y_c = b' + b_l + d_{\text{lat}}. \quad (11)$$

Let us denote the time y_c is attained as t_c.

Theorem 1. *Equation* (11) *gives a lateral clearance distance sufficient for lateral safety when a swerving vehicle becomes laterally adjacent to another braking vehicle, or any time before.*

Proof. To show lateral safety, we must show that laterally adjacent vehicles are at least d_{lat} from one another, as given in Equation (5). Since the swerving vehicle's lateral speed is variable but nonnegative, a conservative lower bound on its lateral velocity is zero when computing d_{lat}. From assumption 1, since the other vehicle is braking, it is not swerving, and therefore has zero lateral velocity during the swerve. The required d_{lat} can then be computed using Equation (5), taking v_r^{lat} and v_f^{lat} to be zero, and using the parameters $a_{\min}^{\text{lat}}$, $a_{\max}^{\text{lat}}$, and ρ.

For $t < t_c$, the swerving vehicle is not laterally adjacent to the other vehicle, and is laterally safe. For $t \geq t_c$, from Assumption 2, t_c is the time at which the two vehicles are closest while laterally adjacent. From Equation 11, there is at least d_{lat} of distance between the vehicles, and thus they are laterally safe $\forall t \geq t_c$. □

B. Swerving for a Braking Vehicle

We can now use y_c to compute the longitudinal safe distance, $d_{s,b}$, required when swerving to avoid a braking lead vehicle. We wish to do so under the constraints of the bicycle model outlined in Section II-A. In addition, if α denotes the lane width, t_f denotes the end time of the swerve, and the origin of the coordinate frame is at the centre line of the current lane at the rear vehicle's position at $t = 0$, we would like the swerve to satisfy the following boundary conditions:

$$\theta(t_f) = 0, \; y(t_f) = \alpha. \quad (12)$$

However, to compute the optimal swerve maneuver with respect to longitudinal clearance is an optimization problem with no closed form solution [11]. Instead, we can compute a swerve maneuver feasible for the bicycle model, and use that to obtain an upper bound on the actual longitudinal distance required by a swerve constrained by the bicycle model. Further details are present in the reference [21].

As in Equation (4), the lead vehicle is travelling with velocity v_f, and then brakes at $a_{\max,\text{brake}}$ during the entire maneuver. The swerve is preceded by the rear vehicle maximally accelerating during the reaction delay ρ, at which point it begins the swerve maneuver with initial speed $v_{r,\rho}$. To ensure monotonicity in the gap between the rear and lead vehicles, a lower bound on the distance travelled until t_f by the lead vehicle is used, denoted x_f.

The swerve we consider is bang-bang in the steering input with zero longitudinal acceleration, and is illustrated in Figure 4. We denote the longitudinal distance travelled by the swerving vehicle until the swerving vehicle reaches the lateral clearance distance as x_c

For the swerve maneuver, the turning radius of the circular arcs depends on the maximum lateral acceleration, as well as the kinematic limits of the steering angle. The constraints on steering angle and lateral acceleration from (7) give two constraints on the turning radius

$$R_{\min,\delta} = \sqrt{\frac{(l_r + l_f)^2}{\tan(\delta_{\max})^2 + l_r^2}}, \quad R_{\min,a} = \frac{v_{r,\rho}^2}{a_{\min}^{\text{lat}}}. \quad (13)$$

To ensure both constraints are satisfied, we set R_c from (7) to the maximum of the two. From this turning radius, we can compute the steering angle δ_c and the slip angle β_c

$$\delta_c = \tan^{-1}\left(\sqrt{\frac{(l_r + l_f)^2}{R_c^2 - l_r^2}}\right), \quad \beta_c = \tan^{-1}\left(\frac{l_r \tan(\delta_c)}{l_r + l_f}\right). \quad (14)$$

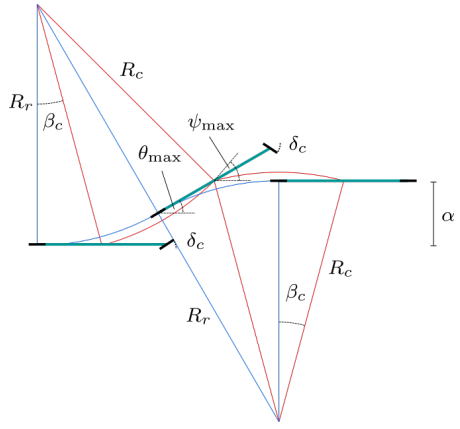

Fig. 4: The swerve maneuver used for safety analysis. The red path is taken by the center of mass, and the blue path is taken by the rear axle. The distance between lanes is α, δ_c is the steering angle, β_c is the slip angle. The maximum angles achieved by the chassis yaw and the velocity of the center of mass are given by $\theta_{\max}$ and $\psi_{\max}$, respectively. The turning radius of the rear axle and center of mass's paths are given by R_r and R_c, respectively.

We can now compute the $\theta_{\max}$ required to satisfy the boundary conditions in Equation (12). From the rear axle, the two circular arcs are symmetrical in lateral distance traveled, as in Figure 4. Therefore, we can compute the angle along the first circular arc required to reach a lateral distance of $\frac{\alpha}{2}$. First, we compute the turning radius at the rear axle, R_r

$$R_r = \frac{l_r + l_f}{\tan(\delta_c)}. \quad (15)$$

Using the value of δ_c computed above, $\theta_{\max}$ is then

$$\theta_{\max} = \cos^{-1}\left(1 - \frac{\alpha}{2R_r}\right). \quad (16)$$

To compute x_c, the longitudinal distance traveled during the swerve, and t_c, the clearance time, there are two cases, depending on if y_c is reached in the first or second circular arc. We can compute $\psi_{\max}$ using (7). From Assumption 3, we have that $\psi_{\max} \leq \frac{\pi}{2}$. Thus, the first case occurs if

$$y_c \leq R_c(\cos(\beta_c) - \cos(\psi_{\max})), \tag{17}$$

otherwise the second case occurs. The equations and derivations of x_c and t_c in each case is given the reference [21].

We can then replace the rear braking distance in Equation (4) with the longitudinal swerve distance x_c. In addition, to ensure a monotonically decreasing gap between the two vehicles, we set the initial speed of the lead vehicle (as a conservative approximation) to

$$v_f' = \min(v_f, v_r \cos(\psi_{\max})). \tag{18}$$

The braking distance of the lead vehicle occurs during the reaction time ρ and the swerve clearance time t_c, giving a front vehicle braking distance of

$$x_f = v_f'(\rho + t_c) - \frac{a_{\max,\text{brake}}(\rho + t_c)^2}{2}. \tag{19}$$

Using the parameters $a_{\max,\text{accel}}, \rho$ introduced in Section II-A, the longitudinal safe distance between a swerving rear vehicle and a braking lead vehicle is

$$d_{s,b} = \left[v_r\rho + \frac{1}{2}a_{\max,\text{accel}}\rho^2 + x_c - x_f\right]_+ + d' + d. \tag{20}$$

Theorem 2. *Equation* (20) *gives a longitudinal safe distance sufficient for safety when swerving for a braking lead vehicle.*

Proof. For $t > t_c$, $y(t) > y_c$, and therefore the swerving vehicle is no longer longitudinally adjacent to the lead vehicle, so is safe from the lead vehicle's braking. For $t \leq t_c$, from Equation (18), we use a conservative lower bound for the speed of the lead vehicle to ensure the lead vehicle's speed is less than the swerving vehicle during the entire swerve. This implies the gap between the two vehicles is monotonically decreasing. This means the minimum gap between the two vehicles occurs at time t_c.

The swerving vehicle travels $x_c + v_r\rho + \frac{1}{2}a_{\max,\text{accel}}\rho^2$, and a conservative lower bound on the lead vehicle's travel distance is $v_f'(\rho + t_c) - \frac{1}{2}a_{\max,\text{brake}}(\rho + t_c)^2$. There is at most d' of distance from the center of mass to the front of the swerving vehicle. Thus, if a swerving vehicle maintains distance $d_{s,b}$, it is safe from the lead vehicle at time t_c. Since the gap is monotonically decreasing for $t \leq t_c$, it is safe $\forall t \leq t_c$. □

C. Braking for a Swerving Vehicle

The longitudinal safe distance required to swerve for a braking vehicle was computed in the preceding section, and this section considers the opposite problem, computing the longitudinal safe distance required to brake for a swerving lead vehicle without collision. Since the lead vehicle intends to occupy the other lane, it requires less longitudinal distance for the rear vehicle to brake to avoid the swerving lead vehicle than it would for it to brake for a braking lead vehicle. We assume the front vehicle is performing the same swerve discussed in Section IV-B. To account for rotation of the front vehicle, $\bar{d}$ is used to compensate as defined in Section IV-A.

We use x_c and t_c from Section IV-B when analyzing the front vehicle's swerve. As in Equation 4, we assume that the rear vehicle accelerates maximally during its reaction time, and then brakes comfortably until t_c. As before, denote the rear vehicle's post-acceleration velocity as $v_{r,\rho}$. Then its minimum velocity during the braking maneuver is

$$v_{r,\min} = \max(\min(v_r, v_{r,\rho} - a_{\min,\text{brake}}(t_c - \rho)), 0). \tag{21}$$

As in Section IV-B, the proof of safety is simplified if the gap is monotonically decreasing until lateral safety is reached. To ensure this, the lead vehicle speed is conservatively bounded with v_f'

$$v_f' = \min(v_f \cos(\psi_{\max}), v_{r,\min}). \tag{22}$$

A conservative lower bound for the longitudinal distance traveled by the swerving front vehicle is then

$$x_f = v_f' t_c. \tag{23}$$

The distance x_f is a lower bound on the distance traveled by the front vehicle during the swerve that creates a monotonically decreasing gap.

The distance traveled by the rear braking vehicle during its reactions delay and its braking maneuver is denoted by x_r. This distance depends on the clearance time t_c, similar to the distance traveled by the front vehicle in the preceding section. The distance traveled during the rear vehicle's braking maneuver, $x_{r,\text{brake}}$, is given by

$$x_{r,\text{brake}} = \begin{cases} v_{r,\rho}(t_c - \rho) - \\ \quad \frac{a_{\min,\text{brake}}(t_c - \rho)^2}{2}, & t_c - \rho \leq \frac{v_{r,\rho}}{a_{\min,\text{brake}}}, \\ \frac{v_{r,\rho}^2}{2a_{\min,\text{brake}}}, & t_c - \rho > \frac{v_{r,\rho}}{a_{\min,\text{brake}}}. \end{cases} \tag{24}$$

Following this, the distance traveled by the braking rear vehicle is

$$x_r = \frac{(v_r + v_{r,\rho})\rho}{2} + x_{r,\text{brake}}. \tag{25}$$

Using Equations 23 and 25, the longitudinal safe distance when braking for a swerving vehicle, $d_{b,s}$ is then

$$d_{b,s} = [x_r - x_f]_+ + d_f + \bar{d}. \tag{26}$$

Theorem 3. *Equation 26 gives a longitudinal safe distance sufficient for safety when braking for a swerving lead vehicle.*

Proof. For $t > t_c$, the swerving vehicle is laterally clear from the rear braking vehicle, and therefore the rear vehicle is safe. The velocity used for the lead vehicle is a conservative lower bound on its true speed $\forall t \leq t_c$, as per Equation 22. In addition, $v_f' \leq v_r$, $\forall t \leq t_c$, and as a result the gap between the two vehicles is monotonically decreasing on that interval. The minimum distance between the two vehicles thus occurs at time t_c. Equation 26 thus gives enough clearance such that no collision occurs at time t_c, so the rear vehicle is safe at time t_c. Since the gap is monotonically decreasing over the interval, the rear vehicle is safe $\forall t \leq t_c$. □

By maintaining a following distance of at least $d_{s,b}$ and $d_{b,s}$ as defined in Equations (20) and (26), we ensure that an autonomous vehicle has enough clearance to be safe from both braking and swerving vehicles. We denote this longitudinal safe distance by $\hat{d}_{\text{long}}$, and it is given by

$$\hat{d}_{\text{long}} = \max(d_{s,b}, d_{b,s}). \tag{27}$$

V. Validation and Results

A. Simulation Setup

In this section, we verify that our kinematic approximation is valid by comparing the longitudinal swerve distance under a dynamic model to the distance computed in the preceding sections. We analyze both the cases when the dynamic model is constrained by $a_{\min,\text{brake}}$ and $a^{\text{lat}}_{\min}$, and when it is not. We wish to show that our acceleration constrained bicycle model swerve distances bound the swerve maneuver distances of a dynamic model employing both swerving and braking whose accelerations are unconstrained by comfort, but instead constrained by feasibility. We would also like to see at which speeds the constrained kinematic bicycle swerve distance is close to the dynamic model swerve distance when the dynamic model is constrained by comfort. We focus on the ability of the dynamic model to swerve, and not an associated controller, and as a result generate the maneuvers in open loop. However, doing a grid search over all possible control inputs to find the best swerves is impractical. Instead, we assume that the steering input is broken into 4 equal length intervals of time, and perform binary search over steering rate magnitudes until the boundary conditions in Equation (12) are satisfied. In addition, we also perform linear search over brake input and the total time of the maneuver and select the maneuver that minimizes the longitudinal swerve distance x_c. Note that these generated swerves are not optimal for the dynamic model, but are feasible.

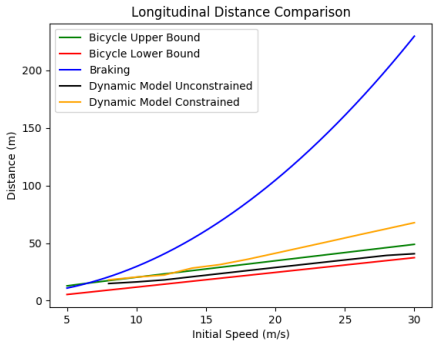

Fig. 5: A comparison of the longitudinal distance traveled during swerve and brake maneuvers, for varying initial velocities. For very low speeds the dynamic model swerves behave poorly and are omitted.

The parameters used in our validation are summarized in Table I. We choose $a_{\min,\text{brake}}$ to represent braking at the limit of comfort, and we choose $a_{\max,\text{brake}}$ to represent a hard, uncomfortable brake. The swerves generated for various initial speeds are illustrated in Figure 6.

TABLE I: Parameters Table

m	1239 kg	l_f	1.19 m	l_r	1.37 m
I_{zz}	1752 kg $\cdot$ m^2	e_{SP}	0.5 m	R	0.302 m
c_w	0.3	ρ_{drag}	1.25 $\frac{\text{kg}}{\text{m}^3}$	A	1.438
B_f	10.96	C_f	1.3	D_f	4560.4
E_f	-0.5	B_r	12.67	C_r	1.3
D_r	3947.81	E_r	-0.5	$a^{\text{lat}}_{\max}$	4.0 $\frac{\text{m}}{\text{s}^2}$
$a^{\text{lat}}_{\min}$	2.0 $\frac{\text{m}}{\text{s}^2}$	$a_{\min,\text{brake}}$	2.0 $\frac{\text{m}}{\text{s}^2}$	μ	0.1 m
$a_{\max,\text{accel}}$	2.0 $\frac{\text{m}}{\text{s}^2}$	$a_{\max,\text{brake}}$	8.0 $\frac{\text{m}}{\text{s}^2}$	ρ	0.1 s
α	3.7 m	d_r	2.3 m	d_f	2.4 m
b_r	0.9 m	b_l	0.9 m	$\delta_{\max}$	$\frac{\pi}{6}$

Using these computed swerves, we then compute the lateral clearance distance y_c as before and find the longitudinal swerve distance traveled x_c that occurs at time t_c. Substituting this value in at Equations (20) and (26) then gives the required longitudinal safe distance for the dynamic model. For the range of initial vehicle speeds where swerving is more efficient than braking, the longitudinal safe distances required for the dynamic model are plotted and compared to those computed in Section IV in Figure 5. We also compare these dynamic model swerve distances to a lower bound on the swerve distance traveled by a bicycle model, which is derived in the reference [21].

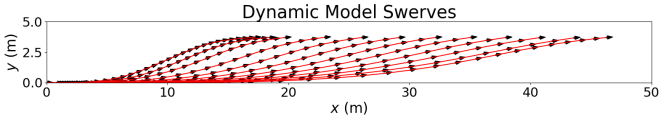

Fig. 6: The swerve maneuvers generated according to the dynamic model. Each swerve is for a different initial speed in the interval [10, 30] $\frac{m}{s}$. The arrows denote the heading of the vehicle.

B. Simulation Results

In Figure 5, we compare the braking distance and the swerve longitudinal distance traveled when avoiding a stationary object. This plot illustrates the advantage of swerves; for initial rear vehicle speeds greater than 8 $\frac{\text{m}}{\text{s}}$, the swerves reach safety using less longitudinal distance than braking does. We note that as $a_{\min,\text{brake}}$ is increased, the crossover point of velocity where swerves become advantageous increases as well. However, due to the quadratic nature of the braking distance, swerves always eventually become more advantageous at high speeds. From the figure, we can see that when the accelerations of the dynamic model are constrained, the swerve distance of the kinematic model is a reasonable approximation of the dynamic model for speeds up to 15 $\frac{\text{m}}{\text{s}}$, with error between 0.7-7.7%, which is reasonable to expect for a kinematic approximation [18]. In the case where the dynamic model is unconstrained by comfort (only by feasibility), the longitudinal swerve distance required is within 15.6-24.0% error of the upper

bound distance of the kinematic model, and is completely bracketed by the kinematic upper and lower bounds across a range of speeds from 8-30 $\frac{\text{m}}{\text{s}}$. This shows that our acceleration constrained kinematic approximation can accurately approximate the swerve distance required by the comfort-constrained dynamic single-track model up to mid-ranged initial speeds, and can bound the swerve distance required by the comfort-unconstrained dynamic model across the entire range of speeds.

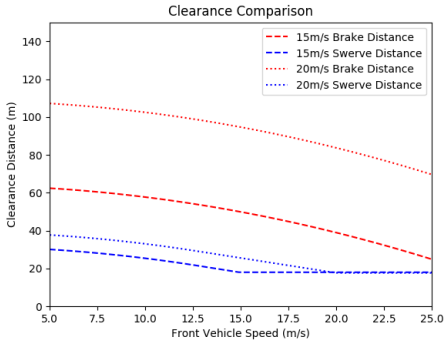

Fig. 7: Comparison between the braking (red) and swerving (blue) distance required when a rear vehicle travels at v_r = 15 $\frac{m}{s}$ (dashed) and v_r = 20 $\frac{m}{s}$ (dotted), as the speed of the front vehicle is varied within the range $[0, 25]\frac{m}{s}$.

In Figure 7, we compare the longitudinal safe distance $\hat{d}_{\text{long}}$ required as clearance for a rear vehicle to swerve or brake for another vehicle in front of it. In the figure, the rear vehicle speed is $v_r = 15\frac{\text{m}}{\text{s}}$ for the dashed lines and $v_r = 20\frac{\text{m}}{\text{s}}$ for the dotted lines. The speed of a front vehicle is varied in the range of $[0, 25]\frac{\text{m}}{\text{s}}$. The braking distances are colored red, and the swerving distances blue. It is clear from the plot that the longitudinal safe distance required when swerving is less than what is required when braking. In fact, swerving allows for a 28-64% reduction in clearance distance when $v_r = 15\frac{\text{m}}{\text{s}}$ and a 65-79% reduction in clearance distance when $v_r = 20\frac{\text{m}}{\text{s}}$. This shows that the required braking distance increases more rapidly than swerving distance does as speed increases, which matches the plot in Figure 5. We note that the swerving distance flattens out once the front vehicle speed reaches the rear vehicle speed due to our conservative bounds, however, it is still lower than the braking distance at said speed.

VI. Conclusions

In this work, we computed safe following distances between vehicles performing brake and swerve maneuvers in a manner similar to that done in the RSS framework. We proved the safety of these following distances under a set of reasonable assumptions about responsible behavior, while incorporating the original assumptions in the RSS framework. In addition, we showed that bicycle model swerve distance bounds the distance required for swerves executed by the dynamic model, validating our kinematic assumptions.

In the future, we would like to extend our work on pairwise safety by computing a following distance that guarantees "utopian" safety similar to that in the RSS framework. We would also like to compare the swerve maneuvers of the kinematic bicycle model with those of a dynamic model that includes pitching, rolling, and combined tire slip. Finally, we would like to extend our work to curved roads.

References

[1] S. Shalev-Shwartz, S. Shammah, and A. Shashua, "On a formal model of safe and scalable self-driving cars," *CoRR*, vol. abs/1708.06374, 2017.

[2] E. Thorn, S. Kimmel, and M. Chaka, "A framework for automated driving system testable cases and scenarios," Virgina Tech Transportation Institute, Tech. Rep. DOT HS 812 623, Sep 2018.

[3] Y. Abeysirigoonawardena, F. Shkurti, and G. Dudek, "Generating adversarial driving scenarios in high-fidelity simulators," *2019 International Conference on Robotics and Automation (ICRA)*, 2019.

[4] M. Althoff, D. Althoff, D. Wollherr, and M. Buss, "Safety verification of autonomous vehicles for coordinated evasive maneuvers," *2010 IEEE Intelligent Vehicles Symposium*, 2010.

[5] M. Althoff and J. M. Dolan, "Online verification of automated road vehicles using reachability analysis," *IEEE Transactions on Robotics*, vol. 30, no. 4, pp. 903–918, 2014.

[6] K. Leung, E. Schmerling, M. Chen, J. Talbot, J. C. Gerdes, and M. Pavone, "On infusing reachability-based safety assurance within probabilistic planning frameworks for human-robot vehicle interactions," *2018 International Symposium on Experimental Robotics*, 2018.

[7] M. Gerdts, "Solving mixed-integer optimal control problems by branch & bound: a case study from automobile test-driving with gear shift," *Optimal Control Applications and Methods*, vol. 26, no. 1, pp. 1–18, 2005.

[8] H. B. Pacejka and E. Bakker, "The magic formula tyre model," *Vehicle System Dynamics*, vol. 21, pp. 1–18, 1992.

[9] C. Schmidt, F. Oechsle, and W. Branz, "Research on trajectory planning in emergency situations with multiple objects," *2006 IEEE Intelligent Transportation Systems Conference*, 2006.

[10] Z. Shiller and S. Sundar, "Optimal emergency maneuvers of automated vehicles," *eScholarship, University of California*, Oct 2005.

[11] ——, "Emergency maneuvers of autonomous vehicles," *IFAC Proceedings Volumes*, vol. 29, no. 1, pp. 8089–8094, 1996.

[12] ——, "Emergency maneuvers for ahs vehicles," *SAE Technical Paper Series*, 1995.

[13] P. Dingle and L. Guzzella, "Optimal emergency maneuvers on highways for passenger vehicles with two- and four-wheel active steering," *Proceedings of the 2010 American Control Conference*, 2010.

[14] Z. Shiller and S. Sundar, "Emergency lane-change maneuvers of autonomous vehicles," *Journal of Dynamic Systems, Measurement, and Control*, vol. 120, no. 1, p. 37, 1998.

[15] H. Jula, E. B. Kosmatopoulos, and P. A. Ioannou, "Collision avoidance analysis for lane changing and merging," *IEEE Transactions on Vehicular Technology*, vol. 49, no. 6, pp. 2295–2308, 2000.

[16] C. Pek, P. Zahn, and M. Althoff, "Verifying the safety of lane change maneuvers of self-driving vehicles based on formalized traffic rules," *2017 IEEE Intelligent Vehicles Symposium (IV)*, 2017.

[17] J. Kong, M. Pfeiffer, G. Schildbach, and F. Borrelli, "Kinematic and dynamic vehicle models for autonomous driving control design," *2015 IEEE Intelligent Vehicles Symposium (IV)*, 2015.

[18] P. Polack, F. Altche, B. Dandrea-Novel, and A. D. L. Fortelle, "The kinematic bicycle model: A consistent model for planning feasible trajectories for autonomous vehicles?" *IEEE Intelligent Vehicles Symposium*, 2017.

[19] J. M. Snider, "Automatic steering methods for autonomous automobile path tracking," Master's thesis, Carnegie Mellon University, 2009.

[20] A. D. Luca, G. Oriolo, and C. Samson, "Feedback control of a nonholonomic car-like robot," *Lecture Notes in Control and Information Sciences Robot Motion Planning and Control*, pp. 171–253, 1998.

[21] R. D. Iaco, S. L. Smith, and K. Czarnecki, "Universally safe swerve manoeuvres for autonomous driving," *arXiv preprint arXiv:2001.11159*, Jan 2020.